Sonel Mapping: A Probabilistic Acoustical Modeling Method

Bill Kapralos[1,2], Michael Jenkin[3,4], and Evangelos Milios[5]

[1]Faculty of Business and Information Technology,
[2]Health Education Technology Research Unit,
University of Ontario Institute of Technology.
2000 Simcoe St. North, Oshawa, Ontario, Canada, L1H 7K4.
bill.kapralos@uoit.ca

[3]Department of Computer Science and Engineering,
[4]Centre for Vision Research,
York University. 4700 Keele St. West, Toronto, Ontario, Canada, M3J 1P3.
jenkin@cse.yorku.ca

[5]Faculty of Computer Science, Dalhousie University.
6050 University Ave. Halifax, Nova Scotia, Canada, B3H 1W5
eem@cs.dal.ca

ABSTRACT

Sonel mapping is a Monte-Carlo-based acoustical modeling technique that approximates the acoustics of an environment while accounting for diffuse and specular reflections as well as diffraction effects. Through the use of a probabilistic Russian roulette strategy to determine the type of interaction between a sound and any objects/surfaces it may encounter, sonel mapping avoids excessively large running times in contrast to deterministic techniques. Sonel mapping approximates many of the subtle interaction effects required for realistic acoustical modeling yet due to its probabilistic nature, it can be incorporated into interactive virtual environments where accuracy is often substituted for efficiency. Experimental results demonstrate the efficacy of the approach.

INTRODUCTION

Given the importance of spatial hearing to humans, incorporating spatialized sound cues in realistic simulations such as immersive virtual environments seems obvious. Spatial sound cues can add a better sense of "presence" or "immersion", they can compensate for poor visual cues (graphics), lead to improved object localization and, at the very least, add a "pleasing quality" to the simulation [1] (a review of spatial sound generation and virtual audio systems is available in [2]). Although the inclusion of such sounds can lead to greater realism and quality, spatial sound cues are often overlooked by the majority of immersive virtual environments where historically, emphasis has been placed on the visual senses instead [3, 4]. Furthermore, when present, the spatial sound cues that are present in these systems do not necessarily reflect natural cues. Many systems that do convey spatial sound information, typically assume that all interactions between a sound wave and objects/surfaces in the environment are specular reflections, despite that in our natural settings, acoustical reflections may be diffuse and there may also be diffractive and refracted components to the sounds we hear as well. Failure to accurately model all these phenomena leads to a decrease in the spatialization capabilities of the system, ultimately leading to a decrease in performance and a decrease in presence or immersion [5].

Simulating the propagation of sound while it interacts with its environment from the time it is emitted from a sound source until the time it reaches a receiver is known as *acoustical modeling.* Acoustical modeling is applied in a wide range of domains from virtual reality to the design and refurbishment of acoustical concert halls, auditoria, and public buildings. The pressure resulting from sound wave propagation can be described by the *wave equation*, also known as the *Helmholtz Kirchhoff equation* [6]. By solving

the wave equation at every time instance and for every position within a particular environment, it is theoretically possible to recover a particular soundfield. Unfortunately an analytical solution to the wave equation is rarely feasible and definitely not applicable to dynamic and interactive virtual environments. As a result, the modeling of the propagation of energy contained in a wave, be it a sound wave or any other type of wave, must be approximated using other techniques.

Sound, just as light, is a wave phenomenon. There are several differences between light and sound including: (i) slower propagation speed of sound, and (ii) wavelength size; the wavelength of most audible sounds is comparable to the size of room surfaces. Although dependent on medium temperature, for most practical purposes, the speed of sound in air can be approximated by 343 $m \cdot s^{-1}$, rather slow when compared to speed of light of 299,792,458 $m \cdot s^{-1}$. When considering light propagation, given the high velocity of light, propagation effects are negligible and it is usually safe to assume propagation is instantaneous in our natural surroundings (except perhaps when considering objects traveling at or near the speed of light). On the contrary, we are clearly capable of detecting (perceiving) the propagation delays of sound as it arrives from the sound source to the receiver both directly and indirectly via reflections. In other words, the arrival time of each reflection is significant and helps to determine the acoustical quality of a particular environment (e.g., size of a room, sound source distance, etc.) [7, 8]. The frequency spectrum of audible sound ranges from approximately 20 Hz to 20 kHz, corresponding to wavelengths ranging from approximately 0.02 m to 17 m. Since, the dimensions of many of the objects/surfaces encountered in our daily lives is within the same order of magnitude as the wavelength of audible sounds, diffraction is an

elementary means of sound propagation especially when there is no direct path between the sound source and the receiver, as is often the case in buildings [9].

Despite the differences, there are also several similarities between light and sound. Computer graphics (image synthesis in particular) and acoustical modeling share many similarities. Both fields model the interaction of waves as they propagate from a source to a receiver, differing only with respect to the type of wave phenomena being modeled. Given the similarities between image synthesis and acoustical modeling, this work investigates the application of suitably modified computer graphics and optics-based modeling methods to model environmental acoustics.

The method developed here is based on photon mapping, a two-pass "particle-based", probabilistic image synthesis method developed by Jensen in 1995 [10]. Photon mapping is a popular image synthesis method and is preferred over finite element techniques such as radiosity for a variety of reasons: It is independent of the scene geometry and thereby allows for the illumination of arbitrarily complex scenes to be computed without having to sub-divide the scene; Furthermore, photon mapping relies on stochastic techniques such as Monte-Carlo integration methods and therefore, the solution can be made more accurate by increasing the number of samples at various points of the computation. In the first pass of photon mapping, "photons" (the basic quantity of light) are emitted from each light source and traced through the scene until they interact with a surface. When photons encounter a diffuse surface, they are stored in a structure called the *photon map*. In the second pass, the scene is rendered using the information provided by the previously collected photon map to provide a quick estimate of the diffuse reflected illumination. Distribution ray tracing is employed to model specular effects. Photon mapping can handle complex interactions between light

and a surface, including pure specular, pure diffuse and glossy reflections, and any combination of them.

This paper describes the *sonel mapping* acoustical modeling method that approximates the time and frequency dependent *echogram* (the temporal acoustical energy distribution) of a particular environment. The echogram can be converted to an equivalent room impulse response function through a post-processing operation [11]. Sonel mapping uses the same basic approach as photon mapping but takes into account the physical attributes of sound propagation, addressing the possible interactions that result when a propagating sound encounters a surface/object or obstruction in its path (e.g., specular and diffuse reflections, diffraction, absorption, and refraction as illustrated in Figure 1). Following the same strategy as used in photon mapping, rather than modeling the exact *mechanical wave* phenomena of sound propagation (e.g., particles in the medium as they move about in their equilibrium position), this process is approximated by emitting one or more "sonic elements/particles" (*sonels*) from each sound source and tracing these sonels through the scene until they encounter an object/surface. A sonel can be viewed as a packet of information propagating from the sound source to the receiver, carrying the relevant information required to simulate mechanical wave propagation.

FIGURE 1 HERE

In addition to modeling specular and diffuse reflections, sonel mapping addresses the modeling of diffraction effects. As previously described, diffraction is a fundamental means of sound propagation, especially when there is no direct path between the sound source and the receiver [13]. Failure to account for diffraction can lead to a non-realistic auditory simulation. Acoustical diffraction with sonel mapping is

approximated using a modified version of the Huygens-Fresnel principle [6]. The Huygens-Fresnel principle assumes a propagating wavefront is composed of a number of secondary sources, fitting nicely into the sonel mapping probabilistic framework whereby acoustical wave propagation is approximated by propagating sound "elements" (sonels). Sonel mapping approximates many of the subtle interaction effects required for realistic acoustical modeling yet due to its probabilistic nature, it can be incorporated into interactive virtual environments where accuracy is often substituted for efficiency.

Paper Organization

The remainder of this paper is organized as follows. Section 2 presents background information on acoustical modeling and in particular, on the methods and techniques used to approximate the room impulse response. In Section 3 sonel mapping is introduced. Details regarding the modifications made to the original photon mapping method to allow for acoustical modeling are given in addition to features such as acoustical diffraction modeling. Experimental results are presented in Section 4 where the outcome of various simulations for various sound source, receiver and occluder configurations is compared to analytical results. Finally, a summary and discussion of future work is presented in Section 5.

BACKGROUND

There are two major computational acoustical modeling approaches: (i) *wave-based* modeling, and (ii) *geometric* modeling.

Wave-Based Room Impulse Response Modeling

The objective of wave-based methods is to solve the *wave equation* in order to recreate a particular soundfield. However, an analytical solution to the wave equation is rarely feasible hence, wave-based methods use numerical approximations such as finite element methods, boundary element methods, and finite difference time domain methods instead [14]. Numerical approximations sub-divide the boundaries of a room into smaller elements. By assuming the pressure at each of these elements is a linear combination of a finite number of basis functions, the boundary integral form of the wave equation can be solved [9, 15]. The numerical computations associated with wave-based methods are prohibitive, rendering them impractical except for the simplest static environments. Aside from basic or trivial applications, such advanced techniques are currently beyond our computational ability for dynamic and interactive applications.

Ray-Based (Geometric) Room Impulse Response Modeling

In a manner similar to geometric optics, with ray-based acoustical modeling it is assumed that sound behaves as a ray and ray-based computer graphics (image synthesis) rendering-like techniques are used to model the acoustics of an environment. Essentially, the propagation paths taken by the acoustical energy are found by tracing (following) these "acoustical rays." Tracing a ray involves following the ray while it propagates from the sound source and interacts with any number of objects/surfaces in the environment before reaching the receiver (listener). Mathematical models are used to account for source emission patterns, atmospheric scattering, and absorption of the sound ray energy by the medium itself and interactions with any surfaces/objects a ray may encounter [16]. At the receiver, the room impulse response is obtained by constructing an *echogram*, which describes the distribution of incident sound energy

(rays) over time. The echogram can be converted to an equivalent room impulse response function through a post-processing operation [17].

Despite being easy to implement, ray-based methods are only valid for higher frequency sounds where reflections are in fact specular. Ray-based methods thus typically ignore the wavelength of sound and any phenomena associated with diffraction. Ray-based methods that do attempt to model non-specular phenomena do so poorly [18, 19, 20]. Failure to accurately model various acoustical phenomena (in particular, diffractive and diffuse components) leads to a decrease in the spatialization capabilities of the system [9, 18, 21]. Another problem associated with ray-based methods involves handling the potentially large number of interactions between a propagating sound ray and any objects/surfaces it may encounter. Upon encountering a surface, a portion of a sound ray's energy may simultaneously be absorbed, reflected both specularly and diffusely, be refracted, and diffracted. Solutions to modeling such effects include emitting several "new" rays at each interaction point (one for each of the interactions). However, such solutions result in excessively large running times and therefore, ray-based methods typically only accurately model the early portion of the room impulse response as they become computationally expensive as the number of reflections increases. Geometric acoustic-based methods include *image sources* [22], *ray tracing* [23], *beam tracing* [9], *phonon tracing* [24], and *sonel mapping* [25, 26].

As an alternative to common deterministic approaches to estimate the type of interaction between an acoustical ray and an incident surface, probabilistic approaches such as a Russian roulette strategy may be used instead. Russian roulette ensures that the path length of each acoustical ray is maintained at a manageable size, yet due to its

probabilistic nature, arbitrary size paths may be explored. Sonel mapping employs a Russian roulette solution in order to determine the type of interaction between a sonel and a surface to determine when the sonel is terminated [27]. Greater details regarding the Russian roulette approach as applied to acoustical modeling is provided in the following sections.

Diffraction Modeling

A number of research efforts have investigated acoustical diffraction modeling. The beam tracing approach of Funkhouser *et al*. includes an extension capable of approximating diffraction [9, 28]. Their frequency domain method is based on the *uniform theory of diffraction* (UTD) [29]. Validation of their approach by Tsingos *et al.* involved a comparison between the actual measured impulse response in a simple enclosure (the "Bell Labs Box") and the impulse response obtained by simulating the enclosure [13].

Tsingos and Gascuel developed an occlusion and diffraction method that utilizes computer graphics hardware to perform fast sound visibility calculations that can account for specular reflections, absorption, and diffraction caused by partial occluders [30]. Diffraction is approximated by computing the fraction of sound that is blocked by obstacles (occluders) between the path from the sound source to the receiver by considering the amount of volume of the first Fresnel ellipsoid that is blocked by the occluders. Rendering of all occluders from the receiver's position is performed and a count of all pixels not in the background is taken (pixels that are "set" e.g., not in the background, correspond to occluders). Although their approach is not completely real-time, unlike other ray-based approaches, it takes advantage of graphics hardware to

operate in an efficient manner. In later work, Tsingos and Gascuel introduced another occlusion and diffraction method based on the Fresnel-Kirchhoff optics-based approximation to diffraction [31]. As with the Huygens-Fresnel approximation, the Fresnel-Kirchhoff approximation is based on Huygens' principle [6]. Comparisons for several configurations with obstacles of infinite extent between their method and between boundary element methods (BEMs) gave "satisfactory quantitative results" [31].

Calamia and Svensson describe an edge-subdivision strategy for interactive acoustical simulations that allows for fast time-domain edge diffraction calculations with relatively low error when compared to more numerically accurate solutions [32]. Their approach allows for a trade-off between computation time and accuracy enabling the user to choose the necessary speed and error tolerance for a specific modeling scenario.

In contrast to the highly physical approaches described here, Martens *et al*. describe a perceptually based solution to the diffraction of sound by an occluder of "low computational cost that is capable of producing distinctive auditory spatial images associated with identifiable effects" [33].

THE SONEL MAPPING METHOD

Sonel mapping traces sound energy propagation from sound sources through the environment (scene) while recording the interaction with any surfaces this energy may encounter in the *sonel map* (see Figure 2(a)). The sonel map is a global data structure that stores acoustical energy (that has been reflected diffusely). The sonel map allows for a very quick estimate of the diffuse sound energy at any point within the model.

The complete energy transmission process is computed by tracing out from the receiver using distribution (Monte-Carlo) ray-tracing coupled with the previously constructed sonel map (see Figure 2(b)).

FIGURE 2 HERE

Prior to beginning the simulation, a description of the model is required. The model description provides information specific to the objects and surfaces comprising the environment including positional information (e.g., three-dimensional surface structure), along with surface characteristic properties (e.g., absorption, diffuse, and specular reflection coefficient values). Sonel mapping can handle arbitrarily complex scenes and models. Sound source distribution functions that describe the frequency, and directional emission patterns of each sound source are supplied in addition to sensitivity functions for each receiver (as commonly done in various acoustical modeling applications, a sphere of radius r_k is used to represent a receiver [34]). For the current implementation, the scene is modeled as a collection of planar, quadrilateral surfaces and each surface is represented by four vertices (v_o, v_1, v_2, and v_3). Being a quadrilateral, each surface contains four edges (e.g., an edge between the vertices v_o and v_1, v_1 and v_2, v_2 and v_3, and v_3 and v_o). A distinction is made between a *diffracting* and *non-diffracting* edge (specified in the scene description). A diffracting edge is an edge where a sonel can be diffracted off of whereas a non-diffracting edge is an edge that is incident on to another surface and therefore a sonel cannot be diffracted off of (see Figure 3).

FIGURE 3 HERE

For the purpose of acoustical diffraction modeling, as shown in Figure 4, each original surface is *dilated* by a frequency dependent amount equal to $\lambda/2$ (where, λ is the

wavelength of the sonel being traced). The dilated surface is divided into two zones: (i) the *diffraction zone*, and (ii) the *non-diffraction zone*. The portion of the dilated surface within a distance of λ of the dilated surface edge comprises the diffraction zone and the remainder of the surface comprises the non-diffraction zone. The types of possible interaction experienced by the sonel when it encounters a surface depend upon which zone the sonel is incident upon. A sonel incident within the diffraction zone is diffracted. A sonel incident within the non-diffraction zone will be reflected either specularly or diffusely or it will be absorbed by the surface.

FIGURE 4 HERE

Sonel mapping is a two-stage algorithm; a *sonel tracing stage* followed by an *acoustical rendering stage*.

> **Sonel tracing stage**: Construct and populate the sonel map by emitting sonels from the sound sources and tracing them through the environment while handling interactions with any objects/surfaces they may encounter.
>
> **Acoustical rendering stage**: Estimation of the echogram using distribution ray tracing from the listener's position, along with the information contained in the previously constructed sonel map.

Stage One: Sonel Tracing

Sound Sources and Emission

Following the common approach in architectural acoustics applications, the distribution of sound frequency in a given sound source is approximated by a fixed number (N_{freq}) of frequencies (63 Hz, 125 Hz, 250 Hz, 500 Hz, 1000 Hz, 2000 Hz, 4000 Hz, and

8000 Hz) [35]. A sound source is specified by its energy distribution function over each of the frequencies and each frequency is considered separately. For each sound source, a pre-determined number of sonels (N_{sonel}) are emitted per frequency band and traced through the environment. The information carried by each sonel includes the information carried by photons in the photon mapping approach: position (*x, y, z* coordinates), direction to incidence and energy, in addition to information specific to sound and sound propagation, including distance traveled, and frequency. The minimum number of sonels N_{min} (e.g., $N_{sonel} \geq N_{min}$) that must be emitted given a receiver represented by sphere of radius r_k is [36]

$$N_{\min} = \frac{4(v_s t_{\max})^2}{r_k^2}, \tag{1}$$

where t_{max} is the echogram duration, and v_s = 343 m·s^{-1} is the speed of sound in air. Each emitted sonel propagates a portion of the sound source energy. Given an omni-directional sound source with a power level of L_s dB (for a particular frequency band), the energy E_{sonel} (W·m^{-2}) of each sonel when emitted from the sound source is given as [37]

$$E_{sonel} = \frac{10^{L/10}}{N_{sonel}} \times 10^{-12}. \tag{2}$$

Sonel-Surface Interactions

When the sonel is incident within the non-diffraction zone, it is either reflected specularly, reflected diffusely, or completely absorbed by the surface. Which of these three interactions occurs is determined using a Russian roulette strategy and thus

collectively decided based upon the value of a uniformly distributed random number $\xi \varepsilon [0 \ldots 1]$ as follows

$$\xi \in [0...\delta] \rightarrow diffuse \tag{3}$$

$$\xi \in (\delta...(\delta + s)] \rightarrow specular \tag{4}$$

$$\xi \in ((\delta + s)...1] \rightarrow absorption \tag{5}$$

where s, and δ are the frequency dependent specular and diffuse surface coefficients respectively. In the event of a diffuse reflection, the sonel is stored in the sonel map and a new sonel is created and reflected diffusely from the sonel/surface intersection point p. When the reflection is specular, a new sonel is created and reflected specularly. In contrast to a deterministic termination criterion, with a Russian roulette approach, the sonel's energy is not attenuated to account for surface absorption when it is reflected. Rather, when the interaction is absorption, the sonel is completely absorbed at the surface and tracing of the incident sonel is terminated.

Specular Reflection

When a sonel is reflected specularly, the sonel is reflected assuming ideal specular reflection whereby the angle of reflection is equal to the angle of incidence. Prior to reflecting the sonel, its relevant parameters are updated to account for the intersection with the surface at point p. This includes adding the distance between the last intersection point and the sonel's current intersection point to the total distance traveled and updating the sonel's current point of intersection (e.g., the incidence point). Storing sonels incident on specular surfaces does not provide any useful information since the probability of having a matching sonel from the specular direction is small (zero for a

perfect specular surface) and therefore, specular reflections are best handled using standard ray-tracing [10].

Diffuse Reflection

When a sonel is reflected diffusely, the information contained in the incident sonel (e.g., the point of interaction on the surface *p*, and distance traveled) is updated and the sonel is stored in the sonel map. A new sonel is then generated and reflected assuming ideal (*Lambertian*) diffuse reflection whereby the reflected direction is perfectly random over the hemisphere surrounding *p* with a probability proportional to the cosine angle with the surface normal [21, 38].

The sonel map represents the sonels that have been reflected diffusely so that they can be used in the acoustical rendering stage to provide an estimate of the statistics of the sound energy contained at each point within the model. As with the photon map used in the photon mapping approach, a *kd-tree* is used to implement the sonel map [39]. A kd-tree with a total of *N* sonels, allows for the localization of sonels in O(N) running time in the worst case, and O(log N) time when the tree is balanced [10]. Once all the sonels in the model have been emitted from the sound source and the sonel map has been populated, the sonel map is balanced thus ensuring O(log N) searches. The balancing operation for a sonel map with *N* sonels has an O(NlogN) running time and in practise may take a few seconds to perform [10]. Provided the sound source remains static in the environment, this cost is incurred once only during the start of the simulation. Any movement of the receiver does not affect the sonel map and therefore, there is no need to update or re-compute the sonel map when only the receiver's position changes.

Diffraction

When the sonel/surface interaction is diffraction, the sonel is propagated in a random direction (θ, φ) over the hemisphere centred on the incidence point (p_{edge}) and whose base is the diffraction surface. Propagating the sonel in the hemisphere surrounding p_{edge} accounts for the fact that the receiver can be positioned anywhere relative to the sound source provided the edge separates them.

Stage Two: Acoustical Rendering

The purpose of the acoustical rendering stage is to estimate the echogram for each of the frequencies considered through the use of the previously constructed sonel map coupled with distribution (Monte-Carlo) ray tracing. N_{rays} frequency dependent acoustical visibility rays are traced from each receiver into the scene. In addition to estimating the diffusely reflected energy (using the sonel map), specularly reflected and diffracted energy is also estimated. As with the sonel tracing stage, any combination of specular reflections, diffuse reflections, and diffraction are accounted for.

Each acoustical visibility ray contains information that describes the total distance it has traveled in addition to its frequency (a discrete set of frequencies are considered as in the sonel tracing stage). During each interaction (intersection) between an acoustical visibility ray and a position p on a surface, the distance between point p and the point p' from which the ray was last emitted/reflected/diffracted from is determined and added to the accumulating distance field of the ray (r_{ray}). When required by the simulation (e.g., when the acoustical visibility ray encounters a sound source (acting as a receiver) and the acoustical visibility ray's energy needs to be added to the accumulating

echogram) the appropriate frequency dependent echogram "bin" (or location) is determined as

$$b_{f_i} = \frac{t_{total}}{t_{rir}}, \tag{6}$$

where b_{fi} represents bin i of the echogram corresponding to frequency f, t_{rir} is the temporal resolution of the echogram (e.g., spacing between "time steps" or "bins") and typically a resolution of about 5-10 ms is sufficient [17]. t_{total} is the total time required for a particular sonel to reach a receiver and is determined by dividing the total path length (distance) r_{total} by the speed of sound v_s = 343 m·s^{-1} (e.g., $t_{total} = r_{total} / v_s$). Prior to adding any energy to the echogram, the energy is scaled to account for attenuation of acoustical energy by the medium (air). Assuming planar sound waves, the attenuation of sound energy due to absorption by the air follows an exponential law [19]

$$E_r = E_o e^{-mr}, \tag{7}$$

where E_o is the original sound energy, E_r is the energy after the sound has traveled a distance r, and m is the air absorption coefficient that varies as a function of the conditions of the air itself (e.g., temperature, frequency, humidity, and atmospheric pressure). Expressions for the evaluation of m are provided by Bass *et al*. [40].

Interactions between an acoustical visibility ray and any objects/surfaces it may encounter are handled in a manner similar to the sonel tracing stage. Upon encountering a surface, a check is made to determine whether the ray/surface incidence

point is within the frequency dependent diffraction or non-diffraction zone. When the ray is within the non-diffraction zone, as in the sonel tracing stage, a Russian roulette strategy is used to determine whether the acoustical visibility ray is reflected specularly, diffusely, or completely absorbed. When the ray is incident within the diffraction zone it will be diffracted off of the edge to which it is closest.

If an acoustical visibility ray encounters a sound source (represented by a sphere of radius r_k for the purposes of this stage), the energy propagating from the sound source to the receiver represented by this particular ray path is scaled to account for attenuation by the medium using eqn (7) with r_{total} assigned the total distance propagated by the acoustical visibility ray. Once the energy has been scaled to account for attenuation by the medium (air), it is added to the accumulating echogram using eqn (6) with t_{total} assigned the value equal to the time taken for the ray emitted by the receiver to reach the sound source.

Direct Sound

Direct sound reaching the receiver is estimated probabilistically during the acoustical rendering stage. When an acoustical visibility ray encounters a surface, a check is made to determine whether the surface belongs to a sound source. If the ray encounters a sound source directly prior to encountering any other surface (e.g., reflection order of zero), then this represents direct sound and a portion of the sound source's energy (the total sound energy divided by the total number of acoustical visibility rays traced from the receiver), is scaled to account for attenuation by the air using eqn (7) (with r_{total} assigned the value of the distance between the sound source and receiver). The scaled

energy is then added to the accumulating echogram using eqn (6) with t_{total} assigned the value of the time taken for the ray emitted by the receiver to reach the sound source.

Specular Reflection

Specular reflections are handled similarly to the sonel tracing stage. When the interaction at the ray/surface interaction point is determined to be specular reflection, the acoustical visibility ray is reflected such that the angle of the reflected ray equals the angle of the incident ray with respect to the surface normal.

Diffuse Reflection

When the interaction between the acoustical visibility ray and the surface at the intersection point p is a diffuse reflection, the acoustical visibility ray is terminated and the sonel map is used to provide an estimate of the sound energy leaving point p. A *nearest neighbor density estimation* algorithm is used to determine the diffuse energy component [41]. An estimate of the energy at point p is made by averaging the energy of the n nearest sonels neighboring point p that are stored in the sonel map. This involves searching through the kd-tree that implements the sonel map for the n sonels that are located within a circle of radius r_s centered about the incidence point p on the surface.

The total path length (r_{total}) is equal to the total distance traveled by the acoustical visibility ray (denoted by r_{ray}) in addition to the total distance previously traveled by the sonel r_{sonel} ($r_{total} = r_{ray} + r_{sonel}$). The energy of each sonel is scaled to account for attenuation by the air using eqn (7) (with $r = r_{total}$). The scaled energy of each of the n sonels is then added to the appropriate "bin" b_{fi} of the accumulating echogram using eqn

(6) with t_{total} equal to the sum between the time for the acoustical visibility ray emitted at the receiver to reach point p and the total sonel propagation time.

Edge Diffraction

Given a sound source (S) and receiver (R) in free space (e.g., no obstacles between them), having originated at S at time $t = 0$ with an amplitude E_o, at time t' the wave will have propagated a distance ρ. This expanding wavefront is divided into a number of ring-like regions, collectively known as *Fresnel zones* [6]. The boundary of the i^{th} Fresnel zone corresponds to the intersection of the wavefront with a sphere of *radius* $r_o + i \times \lambda/2$ centered at the receiver where, r_o is equal to the distance between the receiver and the expanding wavefront after it has traversed a distance of ρ from the sound source, and λ is the wavelength of the sonel. In other words, the distance from the receiver to each adjacent zone differs by half a wavelength ($\lambda/2$). The total energy E_t reaching the receiver can be determined by summing the energy reaching the receiver from each zone. This is approximately equal to one half of the contribution of the first zone E_1 (e.g., $E_t \approx |E_1|/2$) [6].

Essentially, given a sound source, receiver, and edge, the energy reaching the receiver is determined by considering the energy arriving at the receiver from the first Fresnel zone as in the unoccluded scenario described above. To account for diffraction effects, a *visibility factor* is introduced. The visibility factor represents the fraction of the first zone visible from the receiver and is denoted by v_1. Positions on the first zone are uniformly sampled and ray casting is used to determine the fraction of the zone visible to the receiver. The total visibility of the zone is equal to the fraction of sampled positions where a clear path between the sampled position and the receiver exists (n_{vis}),

versus the total number of positions sampled (N_{vis}). Greater details regarding the modeling of acoustical diffraction effects with sonel mapping are available in [42].

EXPERIMENTAL VALIDATION

Simulations have been performed with different sound source, receiver, and environmental configurations (e.g., presence or absence of occluders, etc.) and the results of these simulations have been compared to analytical/theoretical results in order to demonstrate that sonel mapping satisfies and conforms to real-world acoustical energy propagation. All of the simulations described in this section were performed using a Linux-based PC with a Pentium III 500 MHz processor and 512 Mb RAM. Unless specified otherwise, the sonel mapping algorithmic parameters used for the simulations are summarized in Table 1.

Parameter	Value
Receiver radius (r_k)	0.15 m
Source power (L_s)	90 dB
Echogram bin spacing (t_{rir})	5 ms
Number of visibility rays (N_{rays})	30

Table 1. Sonel mapping algorithmic parameters for all simulations unless specified otherwise.

Russian Roulette: Comparison to a Deterministic Approach

In this simulation, the applicability and effectiveness of a Russian roulette strategy to acoustical modeling applications is demonstrated. This demonstration is accomplished by comparing the time required to compute reverberation time estimates using an energy discontinuity percentage (EDP) termination criterion (which represents the percentage of the original ray energy that must be lost before the ray is terminated [43]) and a Russian roulette termination criterion. An enclosed environment 4 m × 4 m × 4 m was simulated with a single omni-directional sound source located at coordinates (in

meters) (3.5, 3.5, 3.5) and the receiver was positioned at (1.0, 1.0, 1.0). The absorption coefficient of each surface was set to 0.1 (a single frequency band was considered). The reverberation time as predicted by Sabine's formula (RT_{pre}), taking absorption by the medium into consideration is 1.03 s. Reverberation times were estimated by computing a linear regression on the -5 to -35 dB portion of the decay curve [44]. The decay curve itself was obtained from the echogram using Schroeder's backwards integration method [45].

The difference between the time taken to compute the reverberation time estimate using an EDP termination criterion and then using a Russian roulette termination criterion is taken as the measure of performance in this simulation. As assumed in Sabine's formulation for reverberation time, in this test all reflections were assumed to be diffuse (e.g., a "perfectly diffuse field"). The diffuse reflection coefficient of surface i (δ_i) was obtained as $\delta_i = 1 - \alpha_i$ where, α_i is the absorption coefficient of surface i. The time required to compute the reverberation times using an EDP termination criterion for various EDP values are shown in Table 2 (typical EDP values range from 90 to 99 [43]). For each EDP setting ranging from 90 to 99, the corresponding reflection count ("Ref. Count"), time taken to compute the estimate ("Time"), and the estimated reverberation time ("RT_{60}") are provided.

EDP	Ref. Count (n)	Time (s)	RT_{60}
90.0	17	4.04	0.16
91.0	19	4.52	0.19
92.0	20	4.46	0.19
93.0	21	5.01	0.20
94.0	22	5.26	0.21
95.0	23	5.50	0.22
96.0	25	6.00	0.25
97.0	27	6.53	0.26
98.0	30	7.23	0.30
99.0	36	8.73	0.35

Table 2. Russian roulette simulation: reverberation time estimates using an energy discontinuity percentage (EDP) termination criterion.

For each EDP-based reverberation time estimate, using a Russian roulette termination criterion, the number of sonels initially emitted from the sound source in the sonel tracing stage was adjusted such that the computed reverberation time was equal (within a small error) to the corresponding reverberation time computed with an EDP termination criterion. The number of sonels initially emitted from the sound source during the sonel tracing stage (stage one) was constant (15,000). Similarly, the number of acoustical visibility rays emitted during the acoustical rendering stage (stage two) was also constant at 1000. A summary of the Russian roulette-based results are provided in Table 3 where for each of the estimated reverberation times, the number of sonels required to compute it ("Num. Sonels"), the maximum reflection count ("Max. Ref.") encountered by any of the emitted sonels, the time taken to compute the solution ("Time"), and the percent difference ("% diff.") between the time taken to compute the reverberation time with an EDP termination criterion t_{edp} and the time to compute the reverberation time with a Russian roulette criterion t_{rus} are given (the reverberation time for the 91.0 and 92.0 EDP was 0.19 s and therefore, the corresponding reverberation time estimate using a Russian roulette approach was computed once only). A positive percent difference indicates $t_{edp} > t_{rus}$ and a negative difference indicates $t_{edp} < t_{rus}$. The percentage difference for each entry of Table 3 is positive indicating that employing a

Russian roulette approach resulted in reduced computation time relative to the deterministic EDP approach.

RT_{60}	Sonel Count	Max. Ref.	Time (s)	% diff
0.16	400	63	0.11	3570
0.19	500	81	0.14	3130
0.20	550	83	0.16	3030
0.21	600	66	0.17	2990
0.22	650	81	0.18	2960
0.25	850	73	0.26	2210
0.26	2000	73	0.57	1050
0.30	3000	85	0.85	750
0.35	5000	79	1.43	510

Table 3. Russian roulette simulation: using a Russian roulette termination criterion to obtain the corresponding reverberation times obtained using an EDP termination criterion.

Diffraction

Diffraction by a Non-Infinite Edge

In this simulation, a “non-infinite” occluder with dimensions 2 m × 2 m was placed between the sound source and receiver. The configuration of the sound source, occluder and receiver is illustrated in Figure 5. The position of the sound source remained stationary while the position of the receiver varied in one meter increments across the “y” and “z” coordinates (in meters), beginning at position (85, 75, 75) and ending at position (85, 85, 85). The sound source was positioned such that the y and z coordinates were centered with respect to the y and z coordinates of the edge.

FIGURE 5 HERE

The purpose of this simulation was to examine diffraction effects by considering the visibility of the first Fresnel zone but over a non-infinite plane were sound can be diffracted via any of the four occluder's edges. Since the corresponding wavelength of the frequencies considered are either greater than or less than the dimensions of the occluder, the inverse relationship between diffraction and frequency can be clearly

demonstrated. Sound source energy was divided equally amongst four sonels (e.g., in this simulation, four sonels were emitted from the sound source only). It was assumed each emitted sonel fell incident on one of the four edges of the occluder and centered along the corresponding edge it was incident on (see Figure 5). This, along with the fact that only four sonels were emitted from the sound source ensures observations and conclusions can be made from the results. Assuming such a symmetrical configuration (e.g., each of the four emitted sonels is incident along one of the four edges and centered along the corresponding edge), allows for meaningful comparisons to be made without having to account for different sonel incident positions, etc. In this simulation only edge effects were considered (e.g., no specular or diffuse reflections were considered). Visibility of the first Fresnel zone was calculated by averaging the visibility associated with each of the four edge positions.

The results of this simulation for the 63 Hz, 125 Hz, 250 Hz, 500 Hz, 1000 Hz, 2000 Hz, 4000 Hz, and 8000 Hz frequencies are illustrated in Figures 6 and 7, where the visibility of the first Fresnel zone relative to the receiver is plotted as a function of receiver position. As shown in Figure 6(a), the visibility of the first Fresnel zone for the 63 Hz frequency for each receiver position was equal to one indicating the first Fresnel zone was completely visible to the receiver for all receiver positions. As the frequency was increased, visibility decreased until it became zero beyond 2000 Hz since the first Fresnel zone was completely blocked by the occluder irrespective of the receiver's position (see Figures 7(a)-(d)).

FIGURE 6 HERE

FIGURE 7 HERE

Sonel Mapping as a Whole

In this simulation, sound propagation in the quasi-cubic enclosure illustrated in Figure 8 was simulated in order to examine the effect of altering the number of sonels emitted from the sound source on the recorded echogram. All possible sonel-surface interactions were considered (e.g., specular and diffuse reflections, diffraction and absorption) in any combination. The simulation was performed for the following frequencies: 125 Hz, 250 Hz, 500 Hz, 1000 Hz, 2000 Hz, and 4000 Hz and for 10,000, 100,000, 500,000, 1,000,000 and 2,000,000 sonels emitted from the sound source and a corresponding number of acoustical visibility rays traced from the receiver. For each simulation, the total sound energy (measured in Decibels) arriving at the receiver over a brief interval of time (three seconds) was measured as was the time taken to compute the simulation. The dimensions of the box-like room were 70 m × 15 m × 70 m, the position (*x, y, z* coordinates in meters) of the single omni-directional sound source and single receiver were (15, 10, 55) and (60, 9, 60) respectively. For each frequency band considered, sound source energy was divided equally amongst all emitted sonels. The surfaces of the enclosure (four walls, ceiling, and floor) were each assigned an absorption coefficient value of $\alpha = 0.15$. The diffuse and specular coefficients were set to a value equal to $(1 - \alpha)/2$. A summary of the simulation results are displayed in Figure 9.

FIGURE 8 HERE

FIGURE 9 HERE

Generally, a decrease in sound level was observed as frequency was increased (and hence wavelength decreased). This is to be expected given the inverse relationship between wavelength and diffraction (in the sonel mapping method, as wavelength is

decreased, the surface diffraction zone is decreased and therefore, the likelihood of diffraction also decreases). An increase in receiver sound level was also observed with increasing sonel count (see Figure 9). This is also expected given that the likelihood of a sonel interacting with a receiver as the number of propagating sonels is increased also increases. However, increasing the sonel count leads to a direct increase in the computation time. This is summarized in Table 4, and shows a direct, linear relationship between sonel count and simulation time. Simulation time was computed by averaging the simulation time required for each of the eight frequency channels considered. With the computer used for this simulation, the average time to emit and trace one sonel was approximately 13 ms. It is anticipated that substantial performance improvements can be achieved using a more current computing platform as opposed to the one used to conduct this simulation.

Sonel Count	Time (s)	σ
10,000	1.25	0.05
100,000	13.25	0.05
500,000	66.12	0.45
1,000,000	132.72	0.19
2,000,000	266.07	2.86

Table 4. Results for the simple room simulation: sonel count vs. average simulation time (average of the simulation time required for each of the eight frequency channels considered) along with standard deviation (σ).

CONCLUSIONS

Sonel mapping is the application of the photon mapping technique to acoustical modeling. It uses the same basic approach as photon mapping but takes into account the physical attributes of sound propagation while addressing the possible interactions when a propagating sound encounters a surface/object or obstruction in its path (e.g., specular or diffuse reflection, diffraction or absorption). Sonel mapping is based on Monte-Carlo ray tracing whereby *point sampling* is used to provide an approximation of

the sound energy in a model and instead of relying on a deterministic approach, sonel mapping employs a Russian roulette approach to determine which type of interaction does occur at each sonel/surface interaction point. Using a Russian roulette approach, a single interaction occurs at each sonel/surface interaction point as opposed to multiple interactions inherent with many deterministic approaches. The use of Russian roulette allows for the possibility of exploring arbitrarily long paths that may not necessarily be explored using deterministic approaches. In addition, it avoids the excessively large running times inherent in many deterministic approaches. Moreover, with Russian roulette, the accuracy of the simulation can be improved by increasing the number of samples initially emitted from the sound source. Although this leads to an increase in computation time, an "efficiency vs. accuracy trade-off" argument can nevertheless be made. In addition to modeling specular and diffuse reflections, sonel mapping addresses the modeling of diffraction effects. Acoustical diffraction is approximated using a modified version of the Huygens-Fresnel principle [6]. The Huygens-Fresnel principle assumes a propagating wavefront is composed of a number of secondary sources. This fits nicely into the sonel mapping probabilistic framework whereby acoustical wave propagation is approximated by propagating sonels (sonic elements/particles) from a sound source and tracing them through the environment. Due to its probabilistic nature, sonel mapping can be incorporated into interactive virtual environments where accuracy is often substituted for efficiency.

Although sonel mapping overcomes many of the problems inherent with currently available acoustical modeling systems, there are several limitations associated with the algorithm as currently implemented. Many of these limitations result from the several assumptions that are currently in place and not necessarily related to limitations with the

algorithm itself. For example, for the purposes of modeling diffraction effects, it is currently assumed that the scene is comprised of planar occluders (edges) only (e.g., no curved surfaces) and therefore, any non-planar objects must be approximated with planar surfaces. Furthermore, edges in the scene where a sonel can be diffracted must be explicitly specified by the user. Other limitations associated with the current implementation are related to the simplified sound source distribution functions and the fact that refraction is ignored. Ignoring refraction limits sonel mapping to indoor environments whereby refraction can in fact be typically ignored [12].

Future Work

None of the simulations reported here included human participants despite the fact that the ultimate user of any acoustical modeling application is a human. Although sonel mapping may be correct with respect to physical laws, human auditory perception must also be accounted for as various physical attributes of sound may lead to differing perceptual responses across human observers. In addition, perceptual factors may also dictate that in certain situations, complete accuracy is not necessarily required and a coarse approximation may be sufficient leading to potential increases in efficiencies. For example, Martens has recognized the importance of perceptual effects with respect to auditory displays and examined the deployment of auditory display technology whereby responses are calibrated to actual responses of a the human listener [46, 47]. Given the importance of perceptual factors, future work will include experimental verification of sonel mapping with human participants to determine the effectiveness of the approach to human listeners, the intended target audience. In addition to verification of the approach, human tests may also lead to refinements to the method in order to account for perceptual effects. Human tests may also allow for meaningful

conclusions to be drawn with respect to the “efficiency vs. accuracy trade-off” in order to determine just how many sonels are required to simulate the acoustics of a particular environment.

ACKNOWLEDGEMENTS

The financial support of the Natural Sciences and Engineering Research Council of Canada (NSERC) is gratefully acknowledged.

REFERENCES

[1] Shilling, R. D., and Shinn-Cunningham, B. Virtual Auditory Displays, In Handbook of Virtual Environment Technology, Lawrence Erlbaum Associates, Stanney, K., Mahwah, NJ. USA, 2002.

[2] Kapralos, B., Jenkin, M., and Milios, E. H. Virtual audio systems. Presence: Teleoperators and Virtual Environments, December 2008, (in press).

[3] Doel, K., Kry, P. G., and Pai, D. K. FoleyAutomatic: physically-based sound effects for interactive simulation and animation. Proceedings of the 28th Annual Conference on Computer Graphics and Interactive Techniques (SIGGRAPH) 2001, Los Angeles, CA. USA, August 12-17 2001.

[4] Cohen, M., and Wenzel, E. The Design of Multidimensional Sound Interfaces. In Virtual Environments and Advanced Interface Design, Oxford University Press Inc., Barfield. W., and Furness, T., New York, NY. USA, 1995.

[5] Svensson, U. P., and Kristiansen, U. R. Computational modeling and simulation of acoustic spaces. Proceedings of the 22nd International Conference on Virtual, Synthetic and Entertainment Audio, Espoo, Finland, June 15-17, 2002

[6] Hecht, E. Optics. Pearson Education Inc., San Francisco, CA. USA, fourth edition, 2002.

[7] Begault, R. 3-D Sound for Virtual Reality and Multimedia. Academic Press Professional, Cambridge, MA. USA, 1994.

[8] Carlile, S. Virtual Auditory Space: Generation and Application. R. G. Landes Company, Austin, TX. USA, 1994.

[9] Tsingos, N., Funkhouser, T., Ngan, A., and Carlbom, I. Modeling acoustics in virtual environments using the uniform theory of diffraction. Proceedings of the 28th Annual Conference on Computer Graphics and Interactive Techniques (SIGGRAPH) 2001, Los Angeles, CA USA, August 12-17 2001.

[10] Jensen, H. W. Realistic Image Synthesis Using Photon Mapping. A. K. Peters, Natick, MA.USA, 2001.

[11] Kuttruff, K. H. Auralization of impulse responses modeled on the basis of ray-tracing results. Journal of the Audio Engineering Society, 1993, 41(11), 876–880.

[12] Cremer, L., and Müller, H. A. Principles and Applications of Room Acoustics, volume 1. Applied Science Publishers LTD., Barking, Essex, UK, 1978.

[13] Tsingos, N., Carlbom, I., Elko, G., Funkhouser, T., and Kubli, B. Validation of acoustical simulations in the “Bell Labs Box”. IEEE Computer Graphics and Applications, 2002, 22(4), 28–37.

[14] Savioja, L. Modeling Techniques for Virtual Acoustics. PhD Dissertation, Helsinki University of Technology, Telecommunications Software and Multimedia Laboratory, Helsinki, Finland, 1999.

[15] Nosal, E., Hodgson, M., and Ashdown, I. Improved algorithms and methods for room sound-field prediction by acoustical radiosity in arbitrary polyhedral rooms. Journal of the Acoustical Society of America, 116(2), 2004, 970–980.

[16] Funkhouser, T., Tsingos, N., Carlbom, I., Elko, G., Sondhi, M., West, J. E., Pingali, G., Min, P., and Ngan, A. A beam tracing method for interactive architectural acoustics. Journal of the Acoustical Society of America, 2004, 115(2), 739–756.

[17] Kuttruff, K. H. Auralization of impulse responses modeled on the basis of ray-tracing results. Journal of the Audio Engineering Society, 1993, 41(11), 876-880.

[18] Kleiner, M., Dalenback, D., and Svensson, P. Auralization - an overview. Journal of the Audio Engineering Society, 1993, 41(11), 861–875.

[19] Kuttruff, K. H. Room Acoustics. Spon Press, London, England, fourth edition, 2000.

[20] Lam, Y. W. A comparison of three different diffuse reflection modeling methods used in room acoustic computer models. Journal of the Acoustical Society of America, 1996, 100(4), 2181–2192.

[21] Torres, R. R., Svensson, P., and Kleiner, M. Computation of edge diffraction for more accurate room acoustics auralization. Journal of the Acoustical Society of America, 109(2), 600–610, 2001.

[22] Allen, J. B., and Berkley, D. A. Image method for efficiently simulating small-room acoustics. Journal of the Acoustical Society of America, 1979, 65(4), 943-950.

[23] Krokstad, A., Strom, S., and Sorsdal, S. Calculating the acoustical room response by the use of a ray tracing technique. Journal of Sound and Vibration, 1968, 8(1), 118-125.

[24] Bertram, M., Deines, E., Mohring, J., Jegorovs, J., and Hagen, H. Phonon tracing for auralization and visualization of sound. Proceedings of IEEE Visualization Conference 2005, Minneapolis, MN. USA, October 23-28 2005.

[25] Kapralos, B., Jenkin, M., and Milios, E. Sonel mapping: A stochastic acoustical modeling system. Proceedings of the IEEE International Conference on Acoustics Speech and Signal Processing (ICASSP) 2006, Toulouse, France, May14-19 2007.

[26] Kapralos, B., Jenkin, M., and Milios, E. Acoustical modeling with sonel mapping. Proceedings of the 19th International Congress on Acoustics (ICA) 2007, Madrid, Spain, September 2-7, 2007.

[27] Kapralos, B., Jenkin, M., and Milios, E. Acoustical modeling using a Russian roulette strategy. Proceedings of the 118th Convention of the Audio Engineering Society, Barcelona, Spain, May 28-31 2005.

[28] Funkhouser, T., Tsingos, N., Carlbom, I., Elko, G., Pingali, G., Sondhi, M., and West, J. E. A beam tracing approach to acoustic modeling for interactive virtual environments. Proceedings of the 25th Annual Conference on Computer Graphics and Interactive Techniques (SIGGRAPH 1998), pages 21–32, Orlando, FL. USA, July 19-24 1998.

[29] Keller, J. B. Geometrical theory of diffraction. Journal of the Optical Society of America, 1962, 52(2), 116–130.

[30] Tsingos, N., and Gascuel, J. D. General model for the simulation of room acoustics. Proceedings of the 24th Annual Conference on Computer Graphics and Interactive Techniques (SIGGRAPH) 1997, Los Angeles, CA. USA, August 3-8, 1997.

[31] Tsingos, N., and Gascuel, J. D. Fast rendering of sound occlusion and diffraction effects for virtual acoustic environments. Proceedings of the 104th Convention of the Audio Engineering Society, Amsterdam, The Netherlands, May 16-19 1998.

[32] Calamia, P. T., and Svensson, U. P. Fast time-domain edge-diffraction calculations for interactive acoustic simulations. EURASIP Journal on Applied Signal Processing, Special Issue on Spatial Sound and Virtual Acoustics, 2007. Article ID 63560, 10 pages.

[33] Martens, W. L., Herder, J., and Shiba, Y. A filtering model for efficient rendering of the spatial image of an occluded virtual sound source. Proceedings of the 137th Meeting of the Acoustical Society of America and the 2nd Convention of the European Acoustics Association, page S54, Berlin, Germany, March 14-19 1999.

[34] Xiangyang, Z., Kean, C., and Jincai, S. On the accuracy of the ray-tracing algorithms based on various sound receiver models. Applied Acoustics, 2003, 64(4), 433–441.

[35] Mehta, M., Johnson, J., and Rocafort, J. Architectural Acoustics Principles and Design. Prentice Hall, Inc., Upper Saddle River, NJ. USA, 1999.

[36] Vorländer, M. Simulation of the transient and steady-state sound propagation in rooms using a new combined ray-tracing/image-source algorithm. Journal of the Acoustical Society of America, 1989, 86(1), 172–178.

[37] Yang, L. N., and Shield, B. M. Development of a ray tracing computer model for the prediction of the sound field in long enclosures. Journal of Sound and Vibration, 2000, 229(1), 133–146.

[38] Svensson, U. P., and Kristiansen, U. R. Computational modeling and simulation of acoustic spaces. Proceedings of the 22nd International Conference on Virtual, Synthetic and Entertainment Audio, pages 11–30, Espoo, Finland, 2002.

[39] Bentley, J. L. Multidimensional binary search trees used for associative searching. Communications of the ACM, 1975, 18(9), 509–517.

[40] Bass, H. E., Sutherland, L. C., and Zuckerwar, A. J. Atmospheric absorption of sound: update. Journal of the Acoustical Society of America, 1990, 88(4), 2019–2021

[41] Silverman, B. W. Density Estimation for Statistics and Data Analysis. Chapman and Hall, London, England, 1986.

[42] Kapralos, B., Jenkin, M., and Milios, E. Diffraction modeling for interactive virtual acoustical environment. Proceedings of the 2nd International Conference on Computer Graphics Theory and Applications (GRAPP 2007), Barcelona, Spain, March 8-11 2007.

[43] Dance, S. M., and Shield, B. M. Modeling of sound fields in enclosed spaces with absorbent room surfaces. Part I: Performance spaces. Applied Acoustics, 1999, 58(1), 1–18.

[44] Lam, Y. W. A Comparison of three different diffuse reflection modeling methods used in room acoustic computer models. Journal of the Acoustical Society of America, 1996, 100(4), 2181-2192.

[45] Schroeder, M. R. New method for measuring reverberation time. Journal of the Acoustical Society of America, 1965, 37(3), 409–412.

[46] Martens, W. L. Rapid psychophysical calibration using bisection scaling for individualized control of source elevation in auditory display. Proceedings of International Conference on Auditory Display (ICAD) 2002, pages 1–8, Kyoto, Japan, July 2-5 2002.

[47] Martens, W. L. Psychophysical calibration for controlling the range of a virtual sound source: Multidimensional complexity in spatial auditory display. International Conference on Auditory Display (ICAD) 2001, pages 1–12, Espoo, Finland, July 29 - August 1 2001.

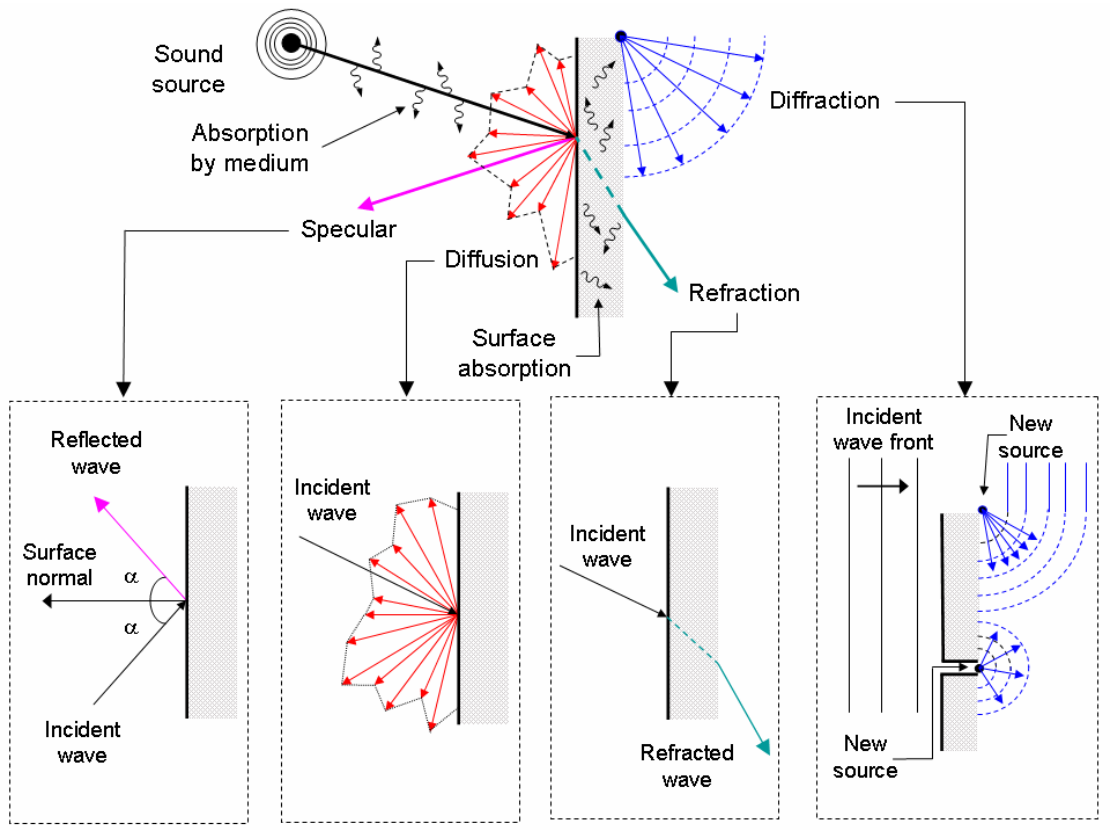

Figure 1. Acoustical reflection phenomena: specular reflection, diffuse reflection, refraction and diffraction. Although refraction can occur, it is not as common as the other interactions when considering room acoustics since even regions in the medium with differing temperatures will eventually inter-mix into a single homogeneous region. Refraction can therefore typically be ignored by room acoustical modeling applications [13].

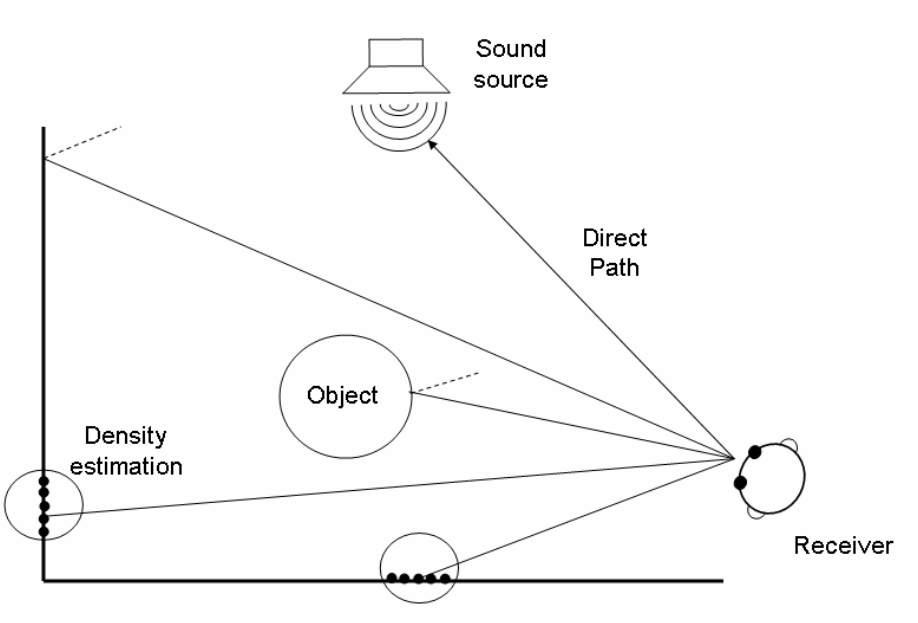

(a) Populating the sonel map.

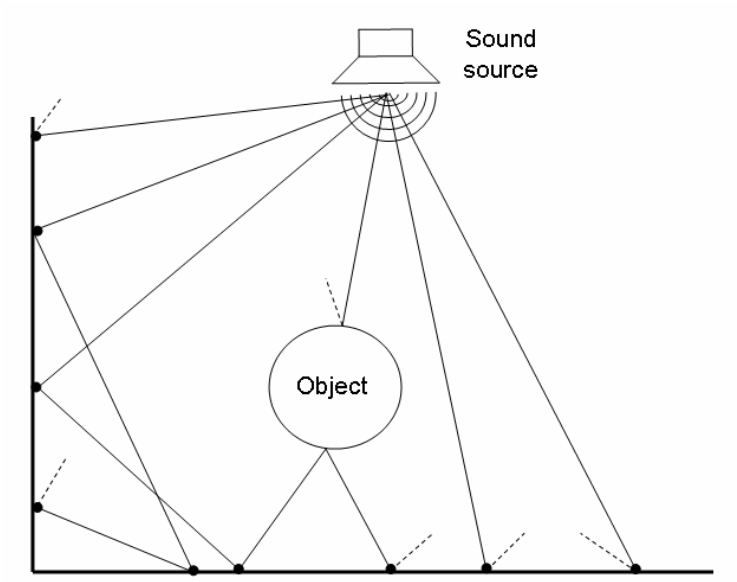

(b) Computing the energy reaching the receiver (echogram).

Figure 2. Sonel mapping. (a) Sonels propagate from the sound sources and traced through the scene while recording the interaction with any objects/surfaces they may encounter. Depending on the type of interaction, sonels may be stored in the sonel map. (b) Once the sonel map has been constructed, the complete energy transmission process is computed by tracing out from the receiver using distribution (Monte-Carlo) ray-tracing coupled with the previously constructed sonel map.

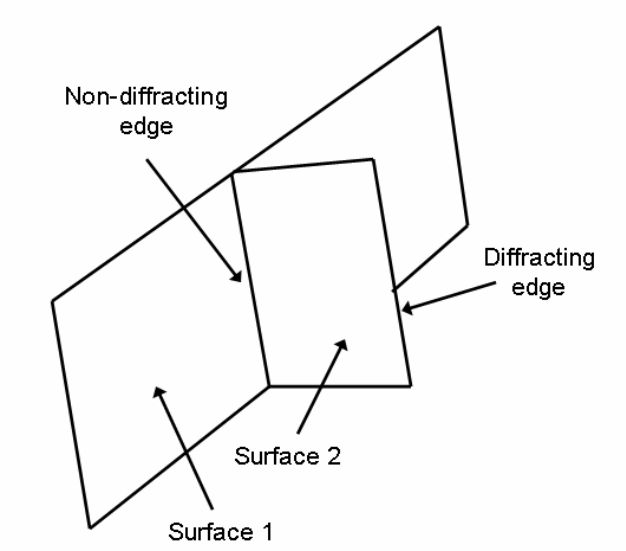

Figure 3. Diffracting and non-diffracting edges defined

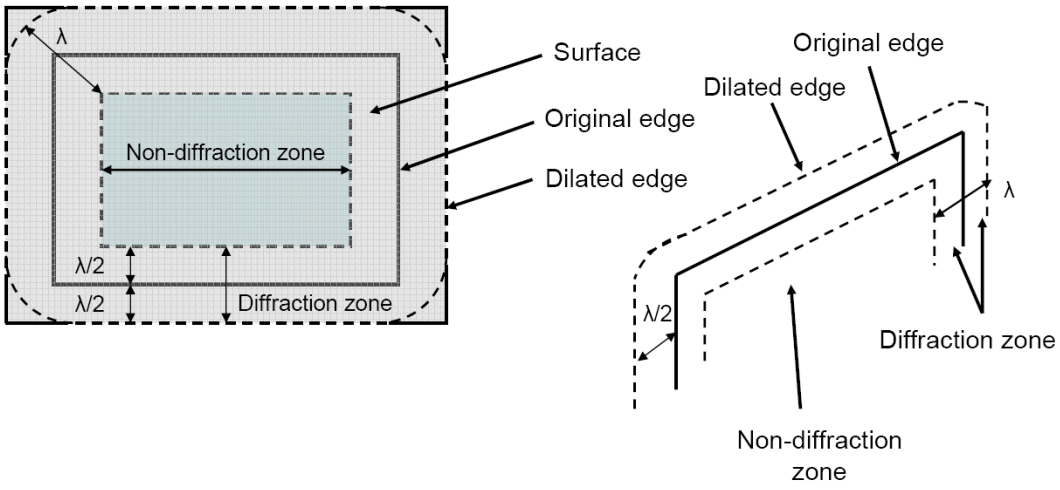

Figure 4. Diffraction and non-diffraction zones defined.

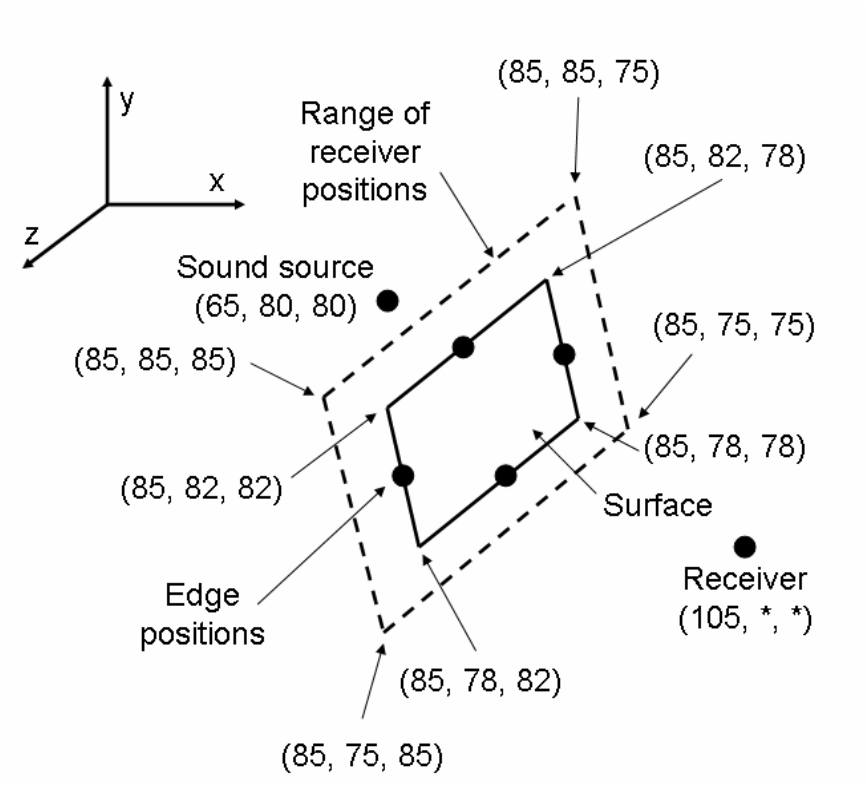

Figure 5. Set-up for the diffraction by a non-infinite edge simulation.

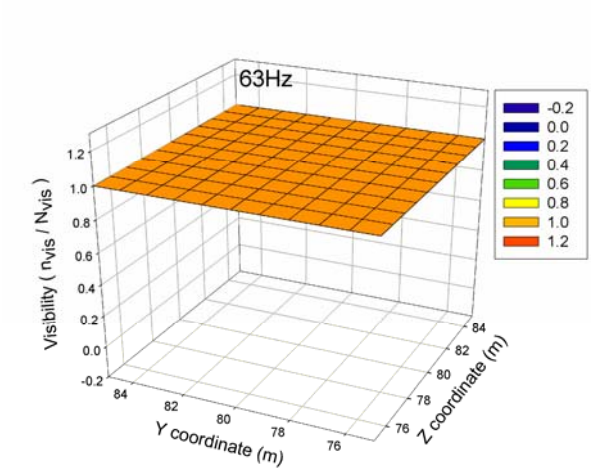

(a) 63 Hz

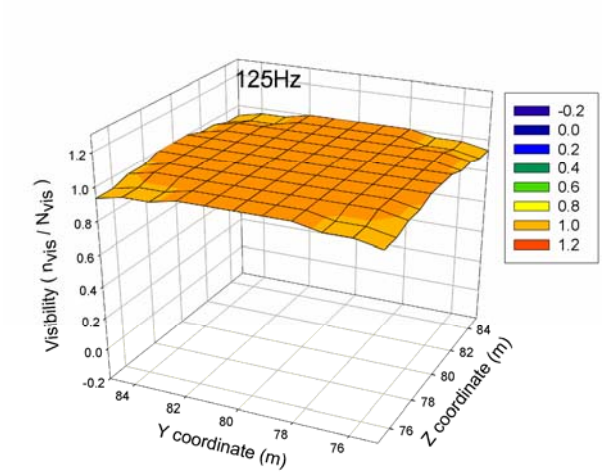

(b) 125 Hz

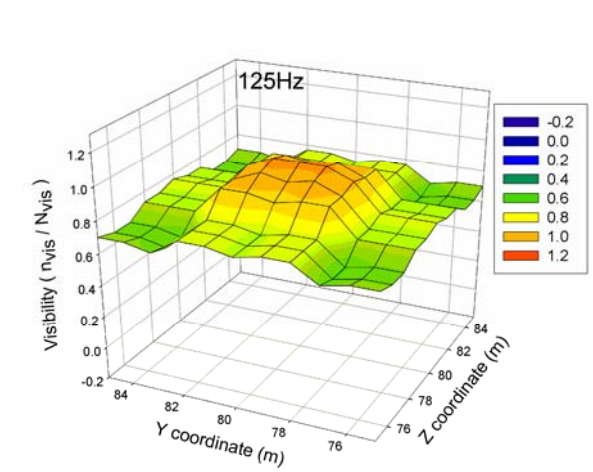

(c) 250 Hz

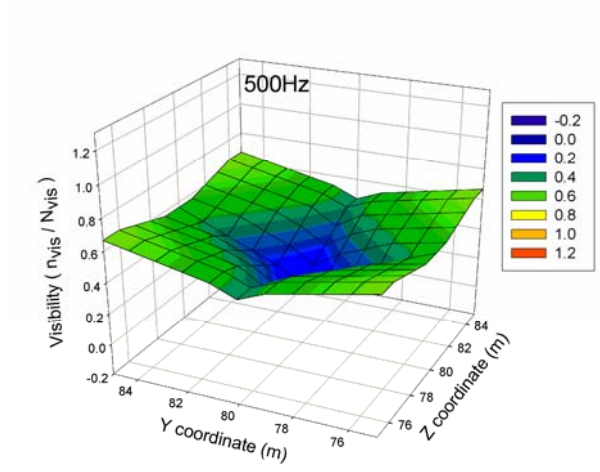

(d) 500 Hz

Figure 6. Diffraction by a non-infinite edge: visibility as a function of frequency. (a) 63 Hz, (b) 125 Hz, (c) 250 Hz, and (d) 500 Hz.

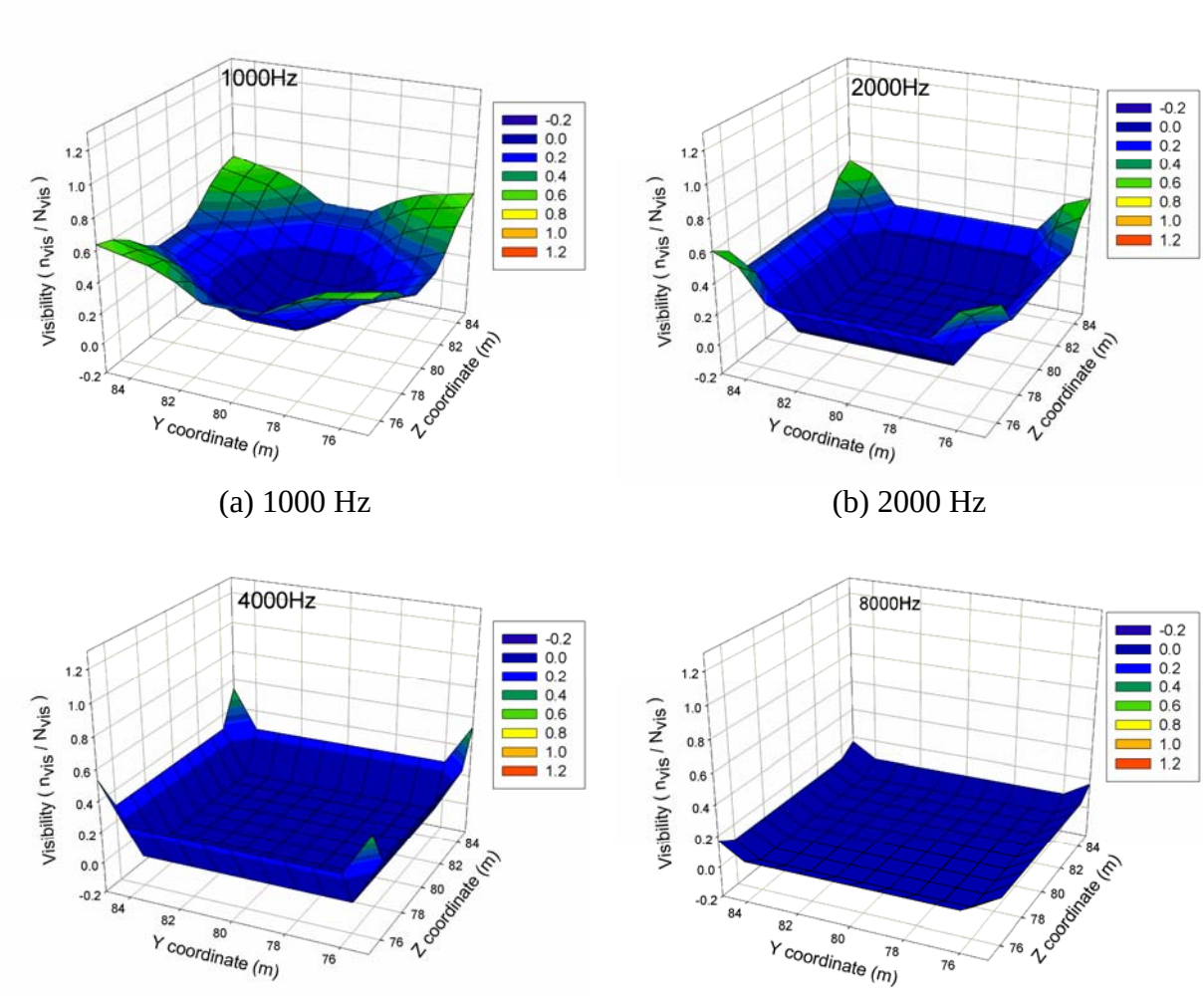

(a) 1000 Hz (b) 2000 Hz

(c) 4000 Hz (d) 8000 Hz

Figure 7. Diffraction by a non-infinite edge: visibility as a function of frequency. (a) 1000 Hz, (b) 2000 Hz, (c) 4000 Hz, and (d) 8000 Hz.

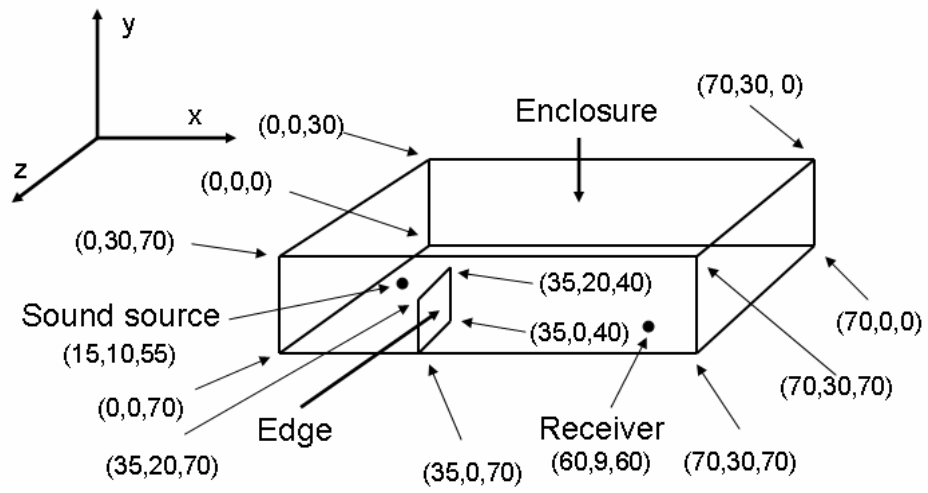

Figure 8. Set-up for the simple room simulation.

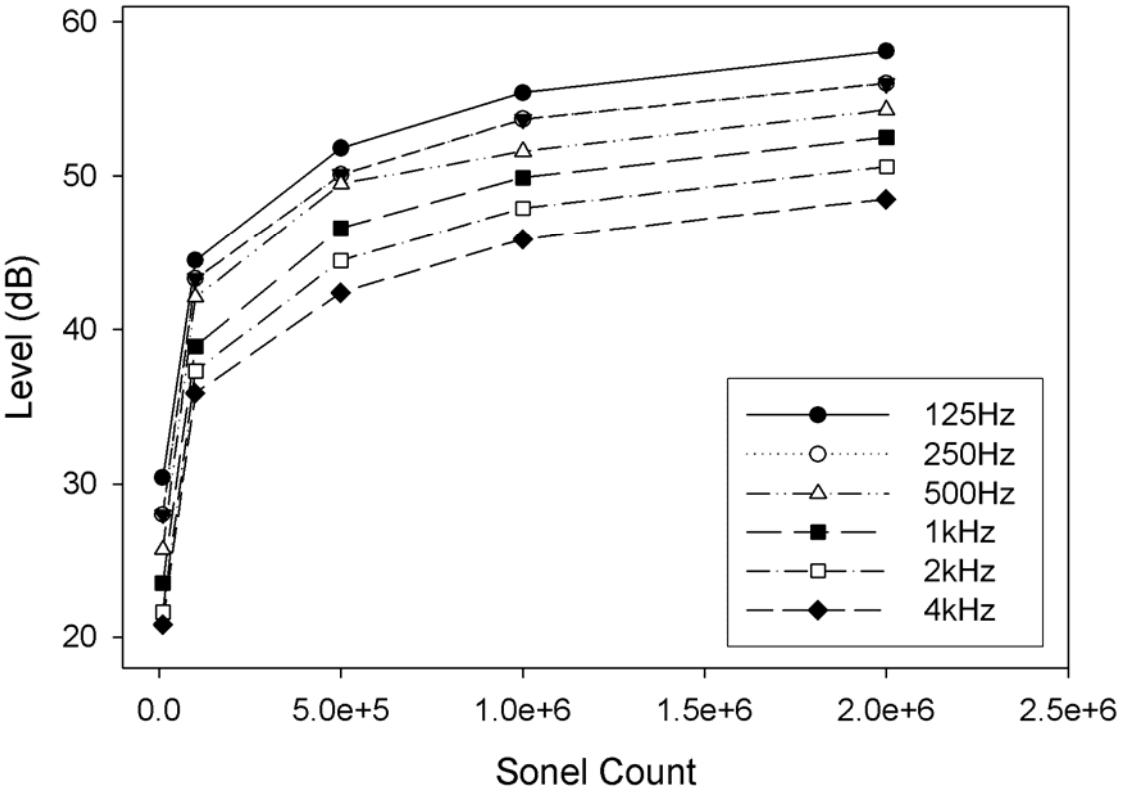

Figure 9. Results for the simple room simulation: receiver level as a function of sonel count for different frequencies.